Solids dynamics in gully pots

Rietveld, Matthijs; Clemens, Francois; Langeveld, Jeroen

DOI
10.1080/1573062X.2020.1823430

Publication date
2020

Document Version
Final published version

Published in
Urban Water Journal

URBAN WATER JOURNAL
2020, VOL. 17, NO. 7, 669–680
https://doi.org/10.1080/1573062X.2020.1823430

Taylor & Francis
Taylor & Francis Group

RESEARCH ARTICLE

OPEN ACCESS Check for updates

Solids dynamics in gully pots

Matthijs Rietveld[a], Francois Clemens[b] and Jeroen Langeveld[a,c]

[a]Faculty of Civil Engineering and Geosciences, TU Delft, Delft, The Netherlands; [b]Department of Hydraulic Engineering, Deltares, Delft, The Netherlands; [c]Partners4UrbanWater, Nijmegen, The Netherlands

ABSTRACT

Runoff entering urban drainage systems contains suspended solids, which carry pollutants and may cause blockages in downstream parts of the system (for example infiltration facilities). Suspended solids inflow should, therefore, preferably be controlled by solids removal at gully pots. This paper presents the results of lab experiments on the solids accumulation in gully pots in a scale 1:1 setup. The accumulation process is initially dominated by settling in the gully pot. When a substantial sediment bed is created, the bed starts to interact with the flow, the removal efficiency of solids decreases, and the bed eventually reaches an equilibrium level. The effects of the discharge, sediment size, and geometry on these processes are assessed. The accumulation rate and equilibrium bed level are strongly affected by the flow pattern which is influenced by the combination of the position the jets impinge on the water and the gully pot's outlet position.

ARTICLE HISTORY
Received 13 March 2020
Accepted 27 August 2020

KEYWORDS
Gully pot; catch basin; sedimentation; urban drainage; experimental research

1. Introduction

A substantial part of urban surfaces is to some extent impermeable. Runoff from these surfaces is usually collected and discharged by drainage systems so as to prevent urban flooding, which may induce substantial damage (Spekkers et al. 2013) and pose public health risks through flooding itself and spreading of pollutants (e.g. De Man et al. 2014), since suspended solids in runoff are known to contain pollutants (e.g. Fulcher 1994; Ashley and Hvitved-Jacobsen 2002). The loading of these solids and their associated pollutants is preferably reduced by interceptors, to avoid blockages in downstream parts of the sewer (e.g., sewer pipes or infiltration facilities) due to sedimentation (Van Bijnen et al. 2018), and to reduce negative environmental impact when discharged into receiving water bodies from storm sewers through storm sewer overflows (SSOs), or from combined sewer systems via combined sewer overflows (CSOs).

The sand trap of a gully pot is such an interceptor. These sand traps have to be emptied regularly to avoid clogging, which would also cause urban flooding and consequently endanger public health (De Man et al. 2014). Post et al. (2016), who monitored the solids accumulation in 300 gully pots over a period of 15 months, developed a statistical model based on field observations in order to determine the timescale for gully pot clogging. Roughly 5% of the gully pots they monitored got progressively filled with solids and eventually got blocked, while the sediment bed levels in the remaining 95% asymptotically grew to a state of equilibrium, indicating that the removal efficiency tends to zero due to an increasing sediment bed level. Consequently, the transport of solids to the drainage system increases over time, which is confirmed by Langeveld, Liefting, and Schilperoort (2016), who showed that the mass of removed solids increased by a factor 3 by cleaning out gully pots six times per year instead of once a year.

Butler and Karunaratne (1995) studied the effect of an increasing sediment bed depth by lab experiments on a gully pot with a sand trap depth of 40 cm and a false bottom to simulate the increasing bed depth. This false bottom was covered with sediment to assess whether the removal efficiency is affected at bed depths of 20, 30, and 40 cm, implicitly assuming a flat sediment bed development. The bed depth hardly affected the removal efficiency and continuous resuspension was only observed for the tests with the smallest particles, highest flow rate, and thickest sediment bed (D_{50} of 68 µm, discharge of 1.5 L/s, and bed height of 40 cm). Sartor and Boyd (1972) simulated the erosion process due to rain storms in gully pots with a substantial sediment bed level. It was found that even in the case of a heavy rain storm lasting 1 h, only about 1% of the mass of the sediment bed undergoes resuspension.

Since the influence of an increasing sediment bed depth on the removal efficiency was found negligible in previous lab experiments, this process was not incorporated in the removal efficiency models found in literature. Lager et al. (1997) found that this removal efficiency is proportional to the diameter of particles, and inversely proportional to the discharge and Grottker (1990) proposed the following empirical relation:

$$\varepsilon = a \cdot Q^b$$

In which ε is the removal efficiency, the parameters a and b depend on the sediment size, Q is the discharge. Butler and Karunaratne (1995) regarded the removal of solids as a trade-off between surface loading and settling velocity. The latter is quantified by application of Stokes' law:

CONTACT Matthijs Rietveld m.w.j.rietveld@tudelft.nl
Supplemental data for this article can be accessed here.

$$\varepsilon = \frac{aw_s}{aw_s + \frac{Q}{A}}$$

$$w_s = \frac{gd^2\left(\frac{\rho_s - \rho_w}{\rho_w}\right)}{18v}$$

In which w_s is the settling velocity, A the free water surface area of the gully pot, d the particle diameter, ρ_w is the density of water, ρ_s is the density of the particle, and v is the kinematic viscosity. The factor a (set at 0.6 to obtain an acceptable agreement with the experimental results of Butler and Karunaratne 1995) accounts for the effect of turbulence, since Stokes' law is applicable for Re<0.1. These two models describe a steady state situation in which the gully pot acts a non-return valve: i.e. it is implicitly assumed that the (growing) sediment bed does not influence the removal efficiency. Butler and Memon (1998) proposed a model which includes resuspension of the sediment bed at the start of the accumulation process, but does not include the effect of a growing sediment bed in later stages. The gully pot is assumed to function a completely mixed reactor in which sedimentation and resuspension occur as described by:

$$\frac{dc_{rs}}{dt} = \frac{Q}{V}(f_{rs}c_{in} - c_{rs}) - \frac{w_{s_{rs}}Ac_{rs}}{V}$$

$$\frac{dc_{ss}}{dt} = \frac{Q}{V}(f_{ss}c_{in} - c_{ss}) - \frac{w_{s_{ss}}Ac_{ss}}{V} + \frac{R}{V}$$

In which c is the concentration, the subscripts rs and ss refer to readily settleable solids and slowly settleable solids, respectively, the subscript in refers to inflow, f is the fraction and R is the resuspension. The description of this resuspension was taken from Fletcher and Pratt (1981), who studied the resuspension of gully pot solids obtained from a gully emptying tanker.

$$R = 0.278 \cdot Q + 2.59 \cdot 10^{-5}\text{fort} < \frac{M_r}{R}$$

In which M_r is the mass of resuspendable solids, which is assumed to be known. All presented models (implicitly or explicitly) assume a completely mixed reactor in which the specific flow pattern (for example affected by the gully pot geometry) does not influence the removal efficiency.

To the authors' knowledge, parameters expected to have a significant influence on the removal efficiency of gully pots, such as an increasing sediment bed depth and the gully pot geometry have not been assessed in detail in literature. Most lab experiments on the removal efficiency found in literature focus on the first phase of the solids accumulation process only and neglect the influence of an increasing sediment bed. Therefore, the work presented here aims to determine, by means of scale 1:1 lab experiments, the importance of an increasing sediment bed on the removal efficiency and assesses the validity of the equation provided by Butler and Karunaratne (1995) for the first phase of the accumulation process.

2. Materials and methods

The experimental setup and procedure are described in section 2.1, the details of the measurement devices are provided in section 2.2, the test conditions are described in section 2.3, and in section 2.4 the post-processing of the measurements is described.

2.1 Experimental setup and procedure

Figure 1 shows the main components of the setup which was used to replicate the sedimentation and erosion processes in a gully pot. The sediment feeder (indicated with the encircled '1' in Figure 1) consists of a tank filled with the sediment selected for the experiment (described in section 2.3.1) and a screw conveyor which is located at the bottom of the tank to regulate the sediment flow. The motor is operated at a constant, controlled speed so as to assure a known supply rate of sediment. The sediment gets suspended in water and is transported through an aluminium canal (with a slope of approximately 1%) to the gully pot (at '2' in Figure 1).

The gully pot is made out of transparent material (PMMA, also known as acrylate) to ensure optical access and its dimensions (at scale 1:1 except from the roughness) are shown in Figure 1(b). The gully pot has a side inlet, in line with the predominant type applied in The Netherlands and is mounted with a height-adjustable bottom as different sand trap depths

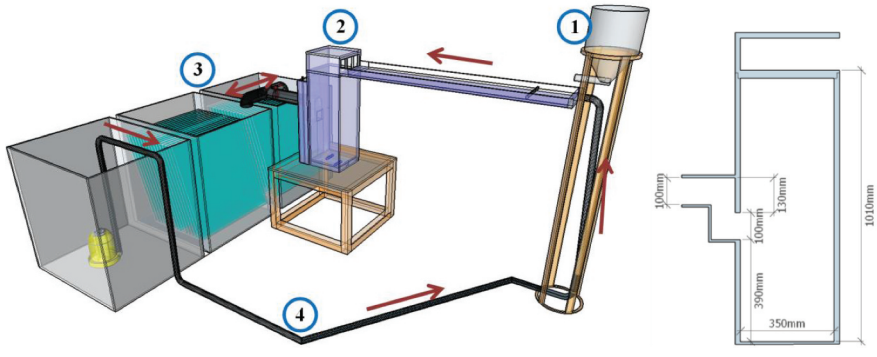

Figure 1. (a). Experimental setup with red arrows indicating the flow direction. (b). Side view of the gully pot including its dimensions. 1. Sediment feeder 2. Gully pot 3. Separation tanks 4. Hose with control valve. 5. Convertible inlet 6. Outlet and siphon 7. Sand trap.

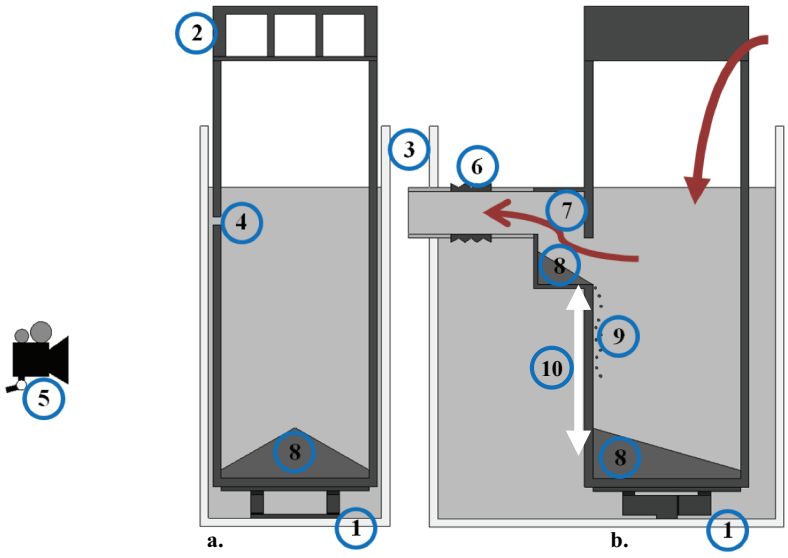

Figure 2. Schematic drawing of the experimental setup with red arrows indicating the flow direction (**a**). Front view (**b**). Side view 1. Weighing scale 2. Gully pot inlet. 3. Surrounding box. 4. Hydraulic connection between gully pot and surrounding box. 5. Camera. 6. Flexible joint. 7. Siphon. 8. Sediment accumulation. 9. Particles sliding out of the siphon into the sand trap. 10. Arrow indicating the mean free depth.

are applied in practice. The inlet (at '5' in Figure 1) splits the water in three jets which impinge on the water in the gully pot. This inlet is convertible to ensure accessibility of the setup (e.g. cleaning or making geometrical changes). The outlet (at '6' in Figure 1) contains a siphon, which in practice acts as a water lock to prevent hindrance due to odours. A butterfly valve is mounted in the outlet pipe of the gully pot, which opening is adjustable to control the water level in the gully pot independent from the discharge. The water level was set at the top of the outlet pipe.

The gully pot is placed on top of a weighing scale, which is used to determine the mass of accumulated solids over time. The sediment that does not settle in the gully pot is transported to two separation tanks (at '3' in Figure 1) and settles there. These two tanks are connected with hoses to a third tank, which contains a pump. This pump recirculates the sediment-free water via another hose (at '4' in Figure 1) to the gully. In this hose, a ball valve and a flow meter (with a straight up- and downstream pipe larger than 10 and 5 times the diameter, respectively) are mounted, which are used to regulate the discharge through the system.

The tests performed were continued until the gully pot's removal efficiency of solids became <10%. To decrease the duration of the tests, the concentration in the inflow was set relatively high, typically 3–4 g/L. It was assumed, based on Butler and Karunaratne (1995), that the removal efficiency is independent from the inflow concentration. The concentration was reduced for the discharges ≤1.0 L/s, since sedimentation would otherwise occur in the aluminium inflow canal. This resulted in test durations ranging from 3.5 up to 38 hours.

2.2 Instrumentation

2.2.1 Flowmeter

The flowmeter is a Fischer and Porter magnetic flowmeter, model D10d, with a measurement range of 0 to 3.5 L/s. The uncertainty (95% confidence interval) of the device is estimated at ±1% of the full scale.

2.2.2 Thermometer

The temperature of the water was measured with a PT100rs thermometer in the tank which contained the pump. The device has an uncertainty <0.05°C, but since the water's temperature in the system wasn't entirely homogeneous, the uncertainty (95% confidence interval) is estimated at ±1°C. The relation between the temperature and the dynamic viscosity is described by Viswanath and Natarajan (1989):

$$\mu = 2.94 \cdot 10^{-5} \exp\left(\frac{508}{T - 149.3}\right)$$

In which μ is the dynamic viscosity and T the temperature. The temperature in all experiments ranged $286 < T < 297$ K, and the viscosity ranged $0.915{\cdot}10^{-6} < \mu < 1.21{\cdot}10^{-6}$ kg·m^{-1}·s^{-1}. The uncertainty has been taken into account when applying Equation 2.

2.2.3 Weighing scale

The mass of the accumulated sediment is determined with a submergible weighing scale, which is shown in Figure 2. This weighing scale was constructed by means of a platform and two Sauter CP 50–3P9 force meters with a range of 500 Newton. The uncertainty (95% confidence interval) specified by the manufacturer is ±0.13 N, which was validated to be correct with calibrated test weights.

The weighing device (indicated with the encircled '1' in Figure 2) was located underneath the gully pot. The gully pot itself was placed inside a PMMA box (at '3' in Figure 2), which was slightly larger than the gully pot itself. To cancel out the hydrostatic pressure in the measurements, the water in the box was hydraulically connected with the water inside the gully pot via small holes in the gully pot wall (at '4' in Figure 2). Small holes are applied to cancel out effects of (slight)

water level variations during the experiments. The observed increase in weight during the experiments represents the weight of the sediment itself minus the buoyancy, allowing to apply force meters with a small range and high precision. The outlet of the gully pot was connected with a flexible joint (at '6' in Figure 2) to the outlet pipe and the gully pot inlet (at '2' in Figure 2) was mounted a few mm above the gully pot, so as to avoid the force on the weighing scale to be affected by disturbances in the inlet or outlet. The removal efficiency of the gully pot is determined using these measurements, and is defined as:

$$\varepsilon = \frac{M_{accumulated}}{M_{supplied}} = \frac{\frac{F_{ws} \cdot \rho_s}{g \cdot (\rho_s - \rho_w)}}{M_{supplied}}$$

In which $M_{accumulated}$ is the mass of the sediment accumulated in the gully pot measured by the weighing scale, $M_{supplied}$ the mass supplied by the sediment feeder, F_{ws} is the force measured by weighing scale, and g is the gravitational acceleration. The supply rate of the sediment feeder is determined by capturing the sediment for a couple of minutes (before the experiment starts) and divide its weight by the time. The uncertainty in the mass supply rate (95% confidence interval) is estimated at ±3% by repeated, independent tests.

The accumulated mass (as measured by the weighing scale) can also be transformed into the depth of the sand trap not occupied by solids, which can be used to compare the results with gully pots with other cross-sectional areas. The free depth (at '10' in Figure 2) is defined as:

$$D_{free} = D - \frac{M_{retained}}{\rho_s \cdot (1 - pr) \cdot A}$$

In which D is the sand trap depth and pr the porosity. The porosity of sand depends on the compaction. Das (2008) reports $0.26 < pr < 0.43$ for coarse sand, but a more precise estimation is made in this study, by comparing the accumulated mass and volume by means of stereo photography of a sediment bed in the gully pot, resulting in a porosity of 0.33 with an estimated uncertainty (95% confidence interval) of ±0.05.

2.3 Test conditions

2.3.1 Solids

In literature, several reports can be found on size distributions of the solids flowing into gully pots. Sansalone et al. (1998) reported $350 < D_{50} < 800$ µm, Pratt and Adams (1984) a D_{50} of approximately 680 µm, and Ellis and Harrop (1984) $600 < D_{50} < 1000$ µm. Gelhardt, Huber, and Welker (2017) reported ρ of approximately 2500 kg/m^3 and Naves et al. (2020) of approximately 2600 kg/m^3 for street solids. To avoid health hazards and for practical reasons, it was decided to use clean sand (ρ approximately 2650 kg/m^3) to mimic real street solids in the experiments. The D_{50}'s used in the experiment were 125, 176, 389, and 1080 µm and the uncertainty (95% confidence interval) in these D_{50}'s is estimated at ±10% of their nominal value. The size distributions are provided in Figure S1 of the Supplementary Material.

2.3.2 Flow

Tests were performed at constant flow rates ranging between 0.35 and 2.0 L/s. This range represents a rainfall inflow intensity between 8.4 and 48 mm/hour (which is comparable to the range tested by Ciccarello et al. (2012)), by dividing the flow rate by a virtual-drained area of 150 m^2 (which is a common value in The Netherlands).

2.3.3 Depth

In practice, gully pots with a range of sand trap depths are applied. The influence of this parameter on the accumulation of solids was tested by adding a (transparent) false bottom. Three different depths were tested namely 0.39, 0.30, and 0.21 m.

2.3.4 Outlet side

Post et al. (2016) found that the orientation of the gully pot outlet (relatively to the inlet) influences the solids build-up in a gully pot. This was assessed in this study by turning the gully pot relative to the inlet by, respectively, 90 and 180 degrees. Figure S2 is included in the Supplementary Material for a graphical representation of the different positions.

2.4 Post processing

The observed sedimentation and erosion phenomena are quantified by means of weight measurements at a frequency of 10 Hz. These measurements show high-frequency noise, which is most-likely caused by vibrations of the setup and water level fluctuations due to the impinging jets. A moving average and moving median filter were applied consecutively to identify the accumulation process in these data. The chosen time window for both filters was chosen such that 0.5 kg of solids was supplied in the time window:

$$t_w = \frac{0.5}{\left(\frac{dM_{supply}}{dt}\right)}$$

Filtering can be applied, since the time window of the filter is substantially shorter than the characteristic time of the accumulation process, which is estimated by an exponential fit of the accumulated mass over time. This characteristic time is for each test at least 70 times larger than the filter time window. The weight measurements over time are also converted into efficiencies over time by Equation 8, which are calculated over a time window which is comparable to a supplied mass of 1 kg.

3. Results and discussion

For brevity, this chapter does not present all the tests. The Supplementary Material contains an overview of the tests in Table S1 and some additional results.

3.1 Preliminary visual observations

A webcam was installed next to the gully pot (perpendicular to the inlet, see Figure 2) to monitor the sediment bed development. Figure 3 shows some characteristic images for a test with a discharge of 1.0 L/s, gully pot depth 0.21 m, sediment size of 389 µm, and the outlet at the back.

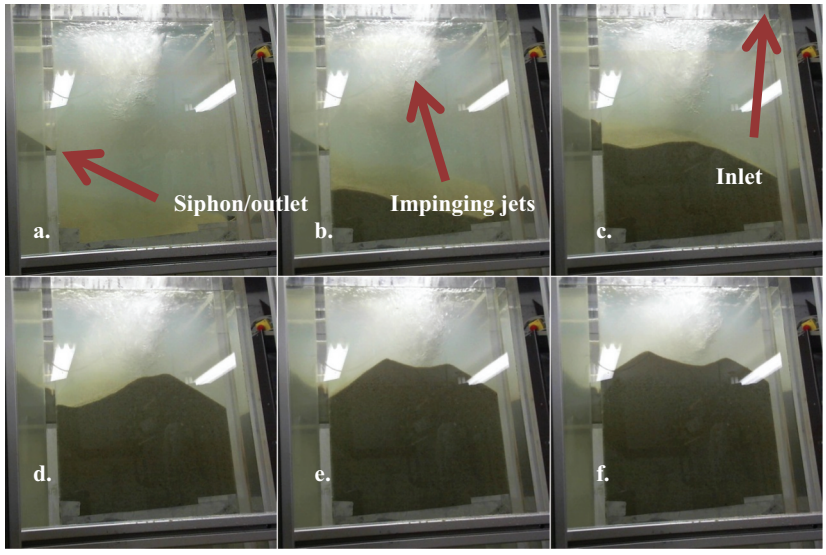

Figure 3. Progressive accumulation of solids over time. (**a**). 1 hour (**b**). 2.5 hours (**c**). 4 hours (**d**). 5.5 hours €. 7 hours (**f**). 8.5 hours.

Figure 3 shows that the sediment bed depth was not uniform over the gully pot's cross section. The shape of the bed depends on the position of the impinging jets, the particle characteristics, and the gully pot geometry. In the first few hours, no resuspension was observed. Particles moved over the sediment as bed load, but already settled particles were not resuspended in the water. Some of the particles that didn't settle in the gully pot, settled in the siphon behind the gully pot (the weight of these particles is included in the weight measurement). These particles reduce the flow area, thus increasing the flow velocity. After some time, resuspension started to occur in the siphon and this bed reached an equilibrium. Sediment was continuously added, transported to the outlet to eventually slide downhill back into the gully pot itself. The latter created an extra hill on the sediment bed below the siphon as indicated in Figure 2.

The three impinging jets originating from the gully pot cause air entrainment (as shown in Figure 3). The sediment bed keeps growing until it gets close to these jets, which cause increased local flow velocities. At this bed level, the effect of the sediment bed on the flow becomes apparent and the accumulation process becomes highly dynamic, particles can be directly transported out of the gully pot, settle in the gully pot, or resuspend from the sediment bed. The sediment bed keeps growing, particularly at locations where it is still relatively thin, resulting in morphological changes (as can be seen in Figure 3(d-f)).

3.2 *Influence of discharge*

The effect of the growing sediment bed and the discharge is quantified by means of weight measurements. The solid line in Figure 4(a) shows the accumulated mass in the gully pot, while the dashed line shows the supplied mass (the measurement methodologies for these masses are described in section 2.2.3). The lines overlap until t is approximately 4.5 hours, implying that nearly all inflowing solids settle in the gully pot. Then, the accumulated mass shows an asymptotic pattern, which means that the efficiency tends to zero. This asymptotic pattern is caused by interaction of the growing sediment bed and the flow. The space not occupied by the sediment bed influences the start of this interaction, which is represented with the parameter free depth, as defined in Equation 9 (since the sediment bed depth is not uniform over the cross section, as shown in Figure 3, it actually represents the mean free depth). Figure 4 (b) shows the removal efficiency for tests at several discharges versus the free depth.

Initially, the removal efficiency of the tests, shown in Figure 4 (b), is relatively constant over the free depth. The fluctuations around these constant values can be caused by imperfections in the construction of the flexible joint (Figure 2), which could cause time lags in the weight measurements due to mechanical shocks caused by sudden lateral movement of the joint, which explains also why the efficiency can temporarily be (significantly) higher than 100% (for the test at 1.0 L/s). At a certain free depth, for example at approximately 0 m for the test at 1.0 L/s, the efficiency decreases almost linearly towards 0%. As described in section 3.1, this is caused by the interaction of the flow with the sediment bed.

Butler and Karunaratne (1995) hardly observed an effect of the bed on the removal efficiency in their setup with an artificially made flat sediment bed at a free depths ≥0 m. In the tests with discharges ≤1.0 L/s the removal efficiency started to decrease at a free depth less than 0 m (and locally an even smaller free depths since the bed was not flat). This might explain why this process was negligible in the tests of Butler and Karunaratne (1995), but not in the experimental results presented here. Free depths less than 0 m (which means that the sediment bed level is higher than the invert level of the outlet) occur in practice (Post et al. 2016), since gully pot maintenance is most often aimed at preventing blockages rather than at reducing the solids loading to the downstream sewer system (Memon and Butler 2002).

Figure 4(b) shows that the discharge is inversely proportional to the removal efficiency (even when the sand trap is empty), since increasing the discharge implies increasing the

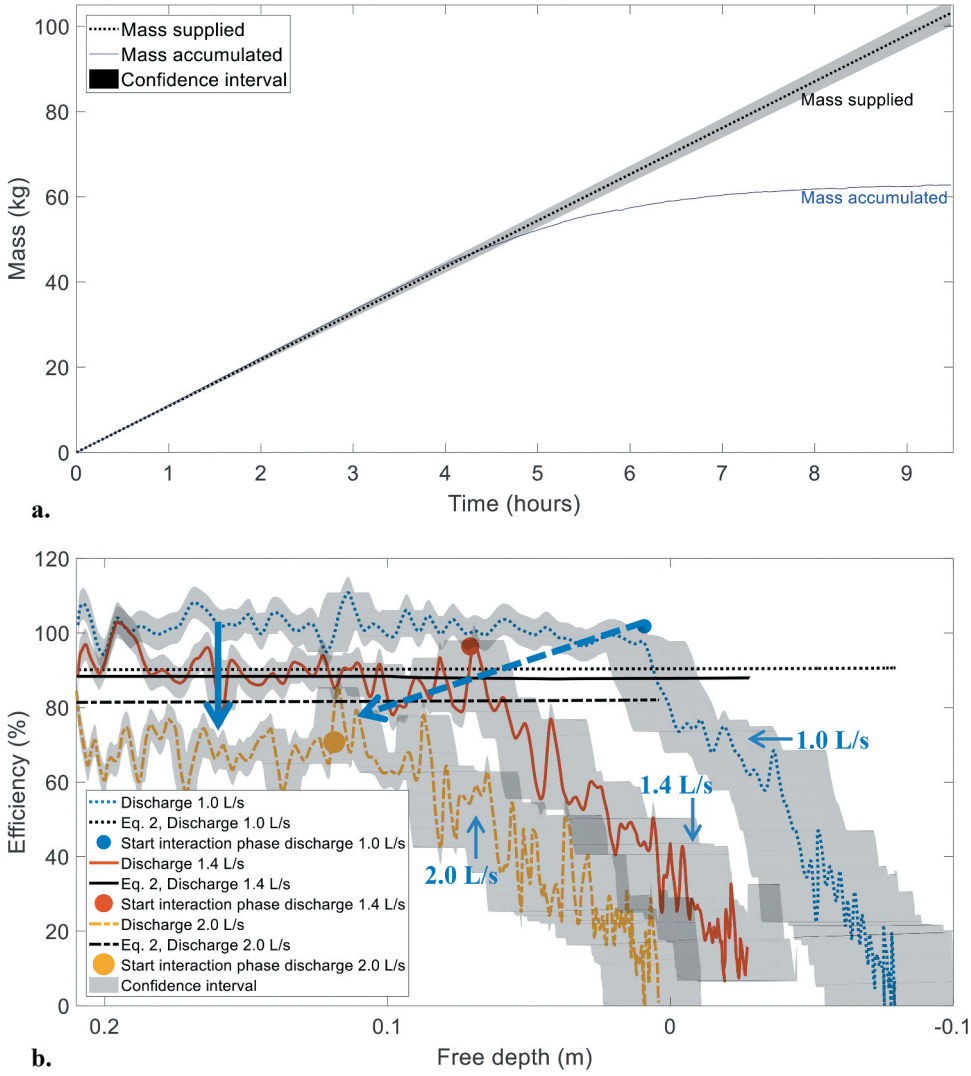

Figure 4. (a).Supplied and accumulated mass over time for test with discharge 1.0 L/s, sand trap depth 0.21 m, sediment size 389 µm, and outlet at the back. Note 1: the confidence interval in the accumulated mass is small and therefore hardly visible. Note 2: the reproducibility of these tests is relatively high, as can be checked in Figure S3 in the Supplementary Material. **(b)**. Measured and theoretical (Butler and Karunaratne 1995) efficiency and $\overline{\varepsilon_1(t_x)}$ versus the free depth for tests at several discharges. The arrows indicate the effect of an increased discharge. The solid arrow indicates a decreased initial efficiency and the dashed arrow indicates a decreased free depth at which the removal efficiency collapses.

inertia relatively to the gravitational force. Moreover, the interaction with the bed starts at lower bed depths at increased discharges, since the shear stress increases with the flow velocity (i.e. discharge). This effect is illustrated in Figure 4(b), as the collapse of the efficiency tends to occur at decreasing values of the free depth with increasing discharge. The increased local flow velocities also reduce the total mass that can accumulate in the gully pot (the retention capacity).

The discharge does not only affect the magnitude of the velocity field but the position where the jets impinge on the water in the gully pot (see Figure 5) as well. At the smallest discharge, the jets stay close to the inlet, while they move closer to the outlet at increased discharges. This affects the morphological evolution of the sediment bed, since it starts building up directly below the inlet at low discharges, and below the outlet at an increased discharge. Furthermore, the intrusion depth of the impinging jet increases with increasing discharge (see Figure 5), which also influences the free depth (Figure 4b) at which the sediment bed starts to influence the removal efficiency.

As discussed, two phases in the solids' accumulation process can be distinguished, which are labelled as non-interaction and interaction phase. The distinction is based on the physical processes, but can be directly linked to the removal efficiency. Almost all tests performed in this research show a constant efficiency during the non-interaction phase and an almost linear decrease of the efficiency during the interaction phase. The starting point of the interaction phase was identified (the black points in Figure 4b) in such a manner that the combined squared error of two linear models, that fit the data at the left and right of this point, was minimised (Equations 11–13).

$$\overline{\varepsilon_1(t)} = \beta_{1,1}t + \beta_{1,0}, t \cdot [0, t_x]$$

$$\overline{\varepsilon_2(t)} = \beta_{2,1}t + \beta_{2,0}, t \cdot [t_x + 1, t_{end}]$$

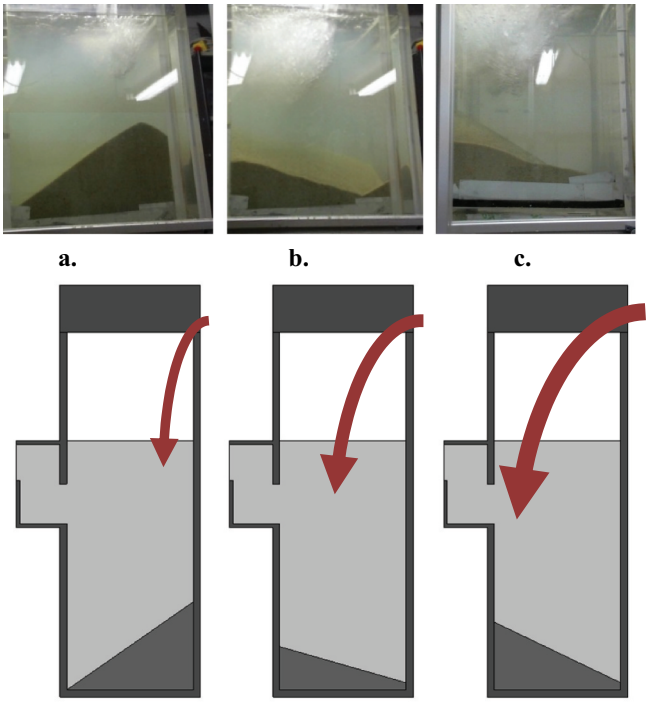

Figure 5. Images and schematic drawings of the sediment bed at different discharges. (**a**). Discharge 0.55 L/s (**b**). Discharge 1.0 L/s (**c**). Discharge 1.8 L/s.

$$\min(SE) = \min_{t_x \cdot [0, t_{end}]} \left(\sum_{t=0}^{t_x} \left(\in(t) - \overline{\in_1(t)} \right)^2 + \sum_{t=t_x+1}^{t_{end}} \left(\in(t) - \overline{\in_2(t)} \right)^2 \right)$$

In which β_i is a coefficient of the linear model and t_x the time at which interaction starts. The identification of the start of the interaction phase by this set of equations should be regarded as an empirical estimation, and not a physical description of the phenomena.

As discussed before, the theoretical efficiency of Equation 2 does not include the effect of a growing sediment bed on the removal efficiency, therefore, this theoretical efficiency is compared with the efficiency measured during the non-interaction phase in Figure 6 (and in similar figures in the next sections). The measured efficiency is significantly larger at discharges ≤1.0 L/s, and significantly smaller at discharges ≥1.8 L/s than the efficiency obtained when applying Equation 2, which was proposed by Butler and Karunaratne.

Memon and Butler (2002) used Equations 4 and 5 to assess the impact of more frequent gully pot cleanings. However, these equations represent mainly the removal efficiency in the non-interaction phase. This means that substantial reduction of the efficiency or even a stabilisation of the sediment bed was not taken into account and one might arrive at the conclusion that more frequent gully pot cleaning hardly affects the suspended solids concentration in storm water. However, Langeveld, Liefting, and Schilperoort (2016) showed that by cleaning out gully pots six times per year instead of once a year, the amount of removed solids increases by a factor 3. This suggests that gully pots operate in the interaction phase in practice. More frequent cleaning would keep them operating in the non-interaction phase, which reduces the solids loading to downstream parts of the drainage system.

3.3 Gully pot depth

The gully pot depth is not included as a parameter in the models proposed for describing the removal efficiency (see section 1.3), and field observations by Post et al. (2016) showed that deeper gully pots retain more solids. Both findings are confirmed by Figure 7(a), which shows tests with different sand trap depths, using the same discharge and sediment size. The graphs start at different free depths due to the different sand trap depths, but do not show significant differences in the removal efficiency. Visual observation also made clear that the development of the shape of the sediment is similar for different gully pot depths. Figure 7(b) shows an overview of initial efficiencies, which makes clear that the discharge significantly affects the efficiency, but the gully pot depth does not.

3.5 Sediments size

The settling velocity, which follows from the application of Stokes' law (shown in Equation 3), depends quadratically on

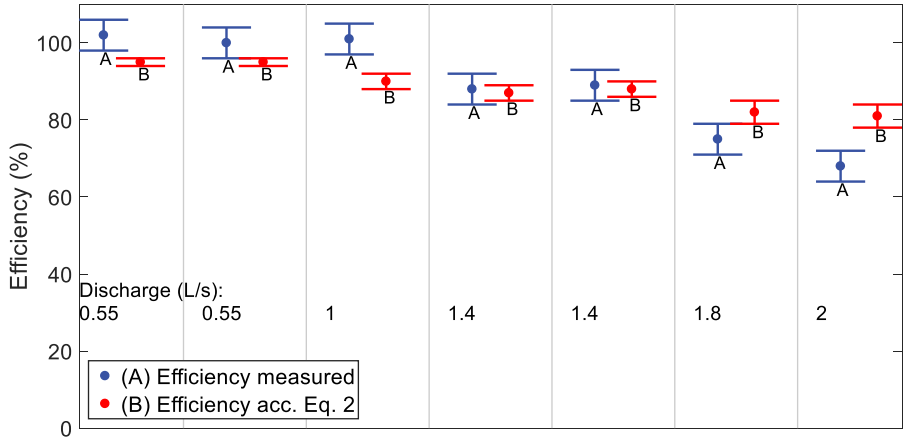

Figure 6. Measured and theoretical (Butler and Karunaratne 1995) efficiency during the non-interaction phase for tests with sand trap depth 0.2 1m, sediment size 389 µm, and outlet at the back (the discharge is defined per column). The whiskers indicate the uncertainty induced by the uncertainty in the weight measurement and mass supply rate for the measured efficiency, and induced by the discharge, temperature/viscosity, and particle size for the theoretical efficiency.

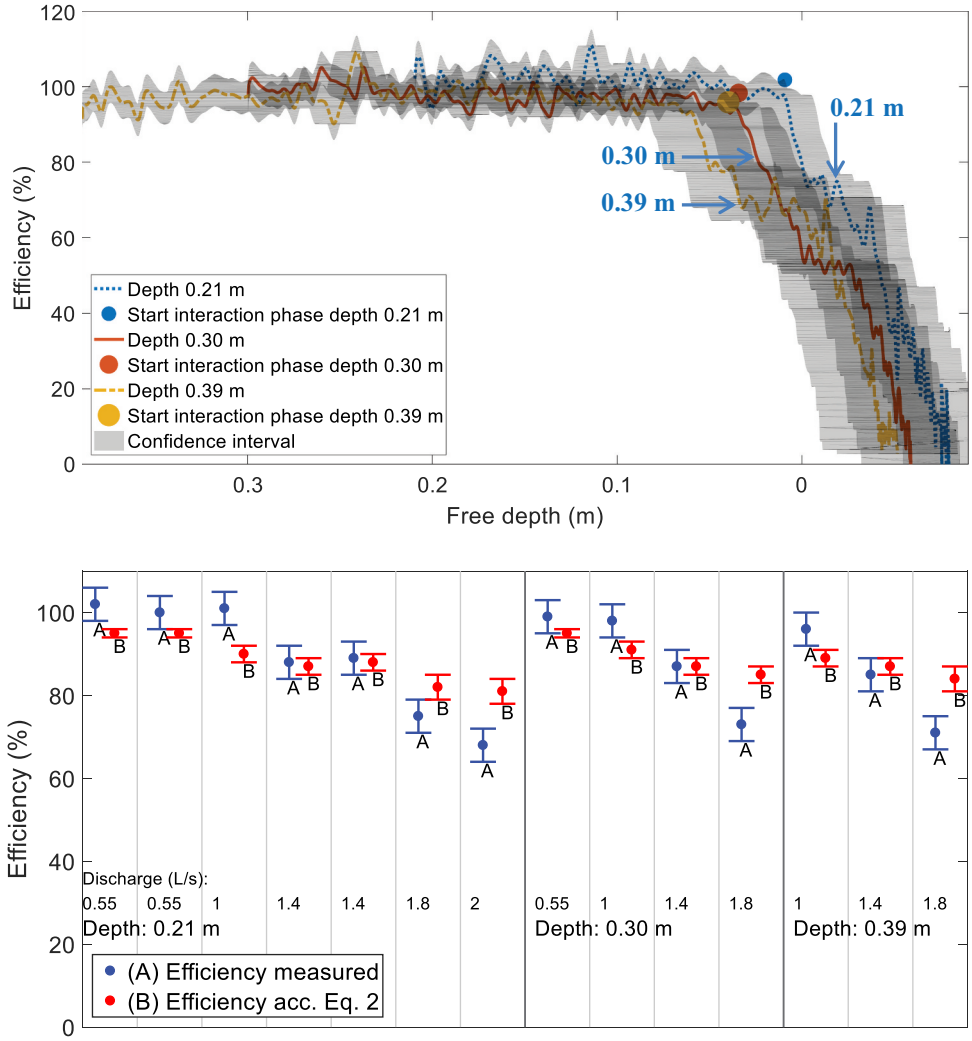

Figure 7. (**a**).Measured efficiency and $\overline{\varepsilon_1(t_x)}$ versus the free depth for tests with sediment size 389 µm, discharge 1.0 L/s, and outlet at the back. **(b)**. Measured and theoretical (Butler and Karunaratne 1995) efficiency during the non-interaction phase for tests with sediment size 389 µm and outlet at the back.

the sediment size. Therefore, the removal efficiency is strongly dependent on the sediment size, as shown in Figure 8(a) for four different grain size fractions at a discharge of 1.0 L/s. For each fraction, the effect of the discharge is similar: it is inversely proportional to the efficiency during the non-interaction phase (as shown in Figure 8b) and inversely proportional to the retention capacity of the gully pot.

Figure 8(b) shows that there are no significant differences between the measured initial efficiencies and the theoretical efficiency for tests with a sediment size of 1080 µm, while significant differences exist for all other sediment sizes, which indicates that the applicability depends on the sediment size. Generally, the impact of the discharge is somewhat stronger than captured in the model. The efficiency is underestimated at low discharges and in some cases overestimated at high discharges.

3.6 Outlet position

The outlet position of the gully pot influences the flow pattern in the gully pot, which consecutively influences the magnitude and direction of the drag force on the particles. Since the gully pot is schematised as a completely mixed reactor in the theoretical equations presented in section 1.1, the effect geometrical changes on the efficiency are not considered as the hydraulics are solely related to the surface loading. In the previous sections, the outlet of the setup was located adjacent to the inlet, at the back of the gully pot. Tests are also performed with the outlet at the front and at the side. In the latter configuration, the flow pattern is likely to represent the most complex, because there is no plane of symmetry.

The accumulation process is strongly influenced by the combination of the position the jets impinge on the water and the gully pot's outlet position. The closer these are together, the lower the removal efficiency, this likely to be caused by the reduction of residence time largely depending on the distance between jet and outlet. Figure 9(a) shows the situation for a discharge of 0.55 L/s. At this discharge, the build-up of the sediment bed starts at the front. If the outlet is also located at the front, the crown of the bed is directly in front of the siphon. The bed partially blocks the outlet, which results in an increased flow velocity and eventually interaction of the bed

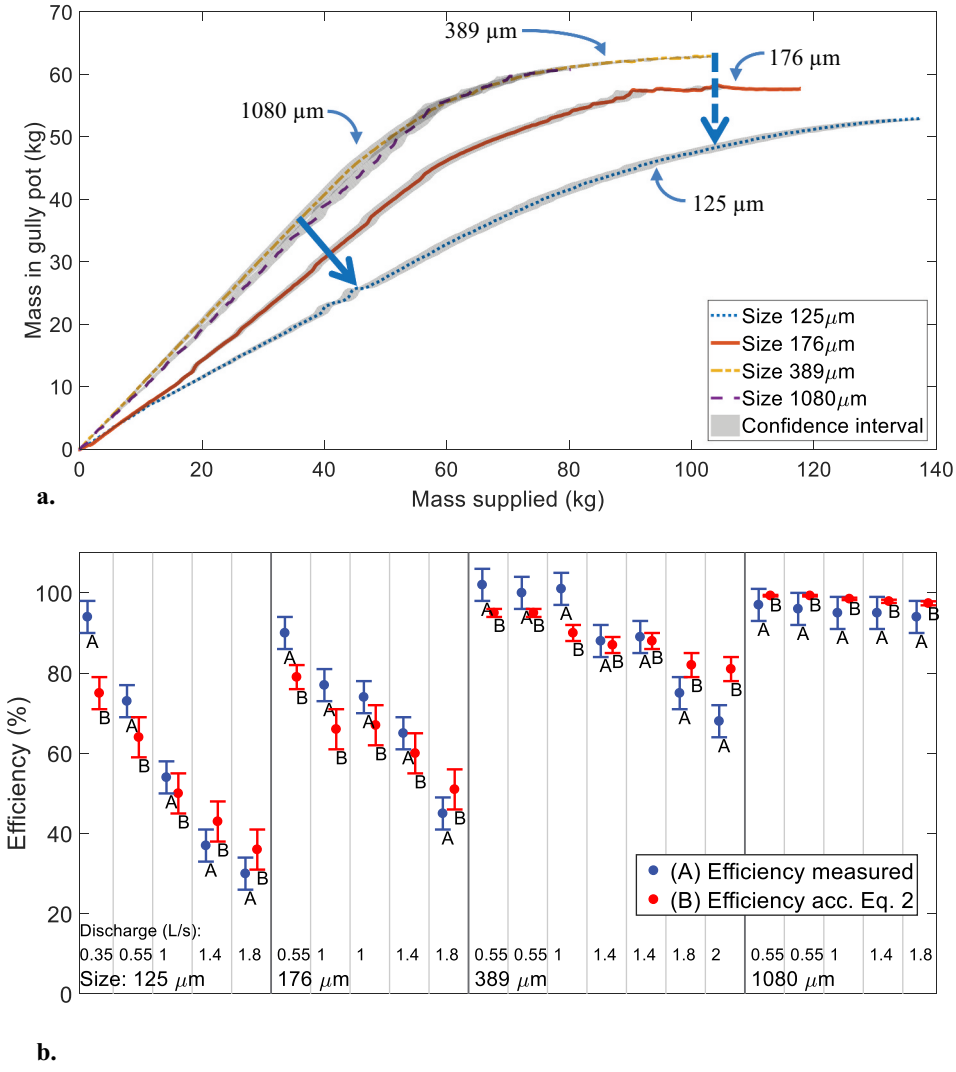

Figure 8. (a). Accumulated mass versus supplied mass for tests with discharge 1.0 L/s, sand trap depth 0.21 m, and outlet at the back. The solid arrow indicates a reduced initial efficiency and the dashed line a reduced retention capacity due to the decreased solids size. (**b)**. Measured and theoretical (Butler and Karunaratne 1995) efficiency during the non-interaction phase for tests with sand trap depth 0.2 1m and outlet at the back.

with the flow. The distance to the outlet is longest if the outlet is located at the back, which results in the latest start of the interaction phase.

At a discharge of 1.0 L/s, the jets impinge on the water in the middle of the gully pot, which is directly in front of the outlet, if it is located at the side (see Figure 9b). This induces immediate transport of suspended solids towards the outlet pipe, resulting in a reduced removal efficiency and retention capacity. At a discharge of 1.4 L/s, the jets are close to the back of the gully pot. Therefore, the removal efficiency and capacity are lowest if the outlet is located at the back, and highest if the outlet is located at the front.

The retention capacity of the gully pot with the outlet at the side was the same at all discharges (except from the lowest discharge). It might be that the local velocities above the sediment bed, and therefore the flow-bed interaction, is dominated by the layout of the gully pot and not by the discharge.

Figure 10 shows that the outlet position induces significant differences in the removal efficiencies. While the efficiency for a gully pot with the outlet at the front is inversely proportional to the discharge (similar to Equation 2), there is no significant relation if the outlet is located at the front, and the relation for an outlet at the side is even more complex. This means that the effect of the distance between the position the jets impinge on the water and the outlet is stronger than the effect of the discharge on the removal efficiency.

4. Conclusions

The sediment bed development in gully pots is initially dominated by settling in the gully pot. This sediment bed develops non-uniformly in depth over the gully pot cross section. The shape of the bed depends on the position of the impinging jet, the particle characteristics, and the flow pattern. In the course of time the evolution of the bed morphology starts to influence the flow field and hence the removal efficiency. Due to increased local velocities and turbulence settling of solids is reduced and solids in the bed can resuspend, eventually the removal efficiency tends to 0%.

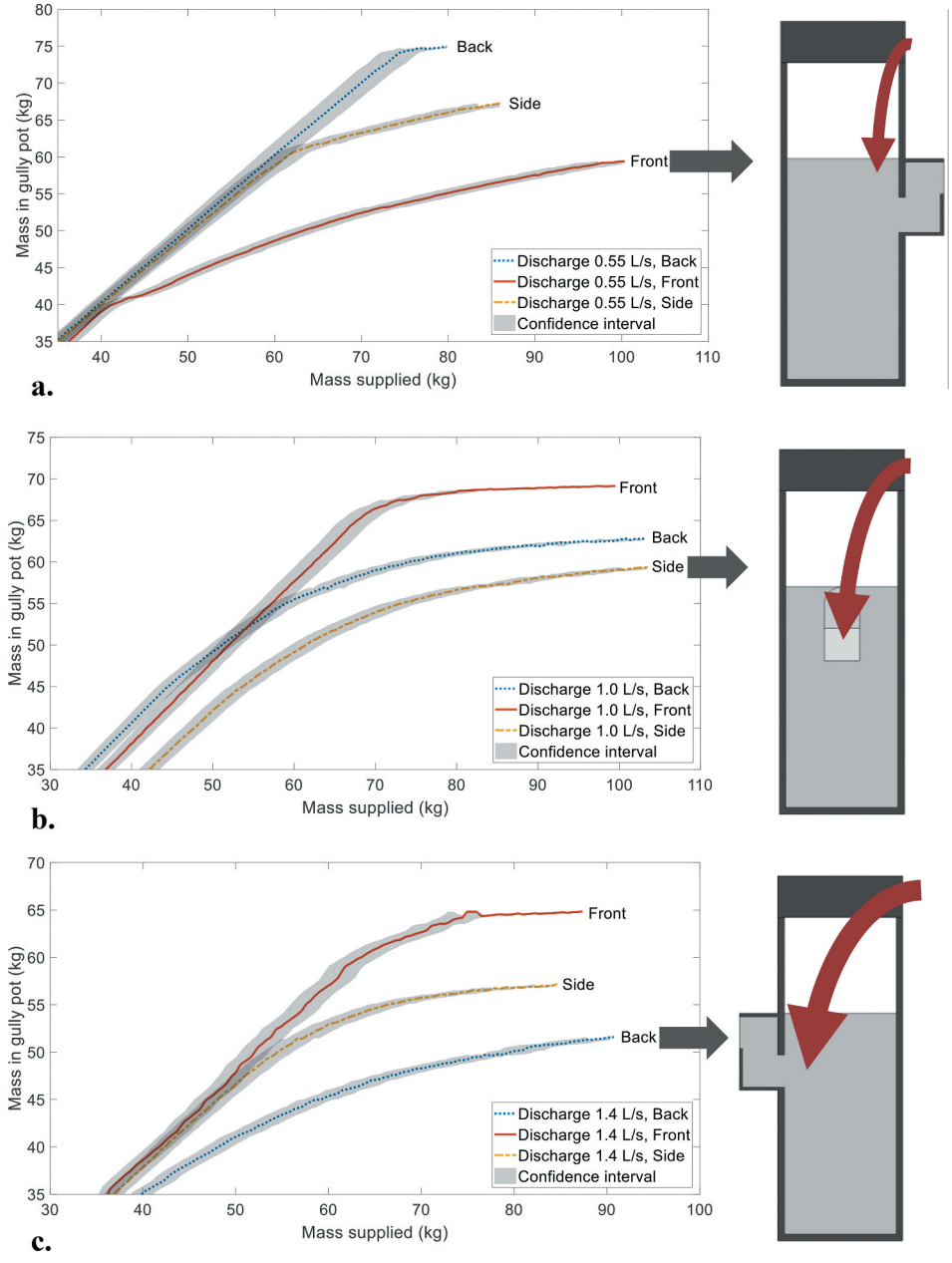

Figure 9. Accumulated mass versus supplied mass for tests with different outlet positions. (**a**). discharge 0.55 L/s (**b**). discharge 1.0 L/s **c**. discharge 1.4 L/s. The drawings at the right indicate for each discharge the outlet position with the lowest removal efficiency.

Apart from the sediment bed depth relative to invert level of the outlet, the removal efficiency depends on the discharge, sediment size, and the geometry. An increased discharge reduces the efficiency and the retention capacity (if the outlet is located at the back), since it increases the inertia relatively to the gravitational force on the solids. The particle size has the opposite effect; larger particles result in an increased removal efficiency and retention capacity. The accumulation process is strongly affected by the flow pattern which is influenced by the combination of the position the jets impinge on the water and the outlet position (Figure 9). The tests with the outlet at the front and at the side show that this effect is, in several cases, stronger than the effect of the discharge on the accumulation process.

The Butler and Karunaratne (1995) equation can be used as a first estimation of the removal efficiency before interaction with the bed starts, but generally underestimates the efficiency at low discharges (< 1 L/s) and sometimes overestimated at high discharges (> 1.8 L/s). Moreover, the calculated efficiencies fit better to the experimental data for larger particles (1080 µm) than for smaller particles (125 µm). The experimental results presented in this study show that the accumulation of solids in a gully pot is a highly dynamic process. The flow pattern and its interaction with the sediment bed are important dynamic processes, influencing the solids' accumulation. A description of these processes is required to improve the efficiency models, such as the Butler and Karunaratne (1995) model.

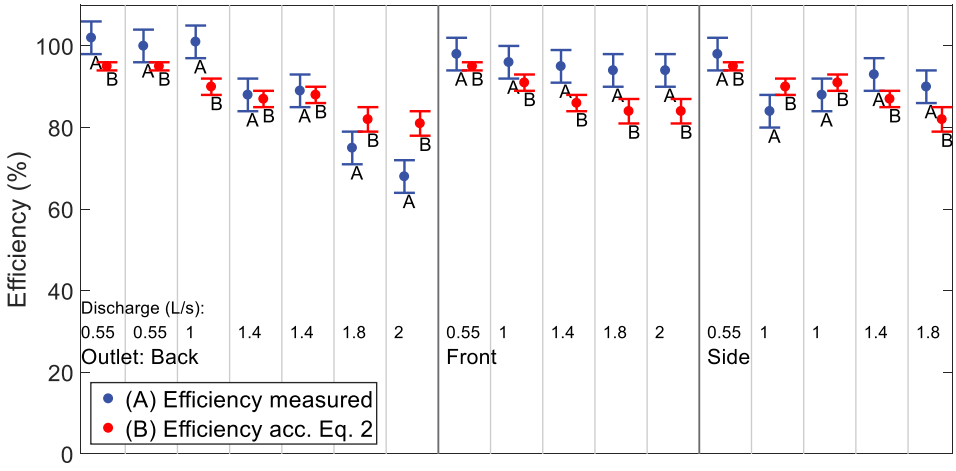

Figure 10. Measured and theoretical (Butler and Karunaratne 1995) efficiency during the non-interaction phase for tests with sand trap depth 0.2 1m and sediment size 389 µm.

The gully pot depth determines when interaction of the bed with the flow starts. A deeper gully pot shows the same removal efficiency, but it takes much longer before the bed reaches the level where interaction with the flow starts. Deeper gully pots could be selected when an urban area is (re)designed, to avoid the necessity of frequent cleanings and thus high cleaning costs, while keeping a high removal efficiency.

List of symbols

a	fitting parameter (-)
A	free water surface area (m^2)
b	fitting parameter (-)
c	concentration ($kg \cdot m^{-3}$)
d	particle diameter (m)
D	sand trap depth (m)
f	fraction (-)
F	force ($kg\ m\ s^{-2}$)
g	gravitational constant ($m \cdot s^{-2}$)
M	mass (kg)
pr	porosity (-)
Q	discharge ($m^3 \cdot s^{-1}$)
R	resuspension ($kg \cdot s^{-1}$)
Re	Reynolds' number (-)
t	time (s)
T	temperature (K)
V	sand trap volume (m^3)
w_s	settling velocity ($m \cdot s^{-1}$)
α	correction factor for settling velocity (-)
β	regression coefficient (-)
ε	removal efficiency (-)
μ	dynamic viscosity ($kg \cdot m^{-1} \cdot s^{-1}$)
ν	kinematic viscosity ($m^2 \cdot s^{-1}$)
ρ	density ($kg \cdot m^{-3}$)

Acknowledgements

The authors thank Deltares for providing the space and practical help to perform the lab measurements. They also thank Carlos Mestre del Pino, who has been working on this project as part of his study curriculum.

Disclosure statement

The authors declare no conflict of interest.

Funding

The research is performed within the Dutch"Kennisprogramma Urban Drainag" (Knowledge Programme Urban Drainage). The involved parties are: ARCADIS, Deltares, Evides, Gemeente Almere, Gemeente Arnhem, Gemeente Breda, Gemeente Den Haag, Gemeentewerken Rotterdam, Gemeente Utrecht, GMB Rioleringstechniek, KWR Watercycle Research Institute, Royal HaskoningDHV, Stichting RIONED, STOWA, Sweco, Tauw, vandervalk+degroot, Waterschap De Dommel, Waternet and Witteveen +Bos

ORCID

Francois Clemens http://orcid.org/0000-0002-5731-0582

References

Ashley, R. M., and T. Hvitved-Jacobsen. 2002. *Management of Sewer Sediments*. Boca Raton: CRC Press/Lewis Publishers.

Butler, D., and F. A. Memon. 1998. "Dynamic Modelling of Roadside Gully Pots during Wet Weather." *Water Research* 33 (15): 3364–3372. doi:10.1016/S0043-1354(99)00050-0.

Butler, D., and S. H. P. G. Karunaratne. 1995. "The Suspended Solids Trap Efficiency of the Roadside Gully Pot." *Water Research* 29 (2): 719–729. doi:10.1016/0043-1354(94)00149-2.

Ciccarello, A., A. Bolognesi, M. Maglionico, and S. Artina. 2012. "The Role of Settling Velocity Formulation in the Determination of Gully Pot Trapping Efficiency: Comparison between Analytical and Experimental Data." *Water Science & Technology* 65 (1): 15–21. doi:10.2166/wst.2011.775.

Das, B. M. 2008. *Advanced Soil Mechanics*. London: Taylor & Francis.

De Man, H., H. H. J. L. Van den Berg, E. J. T. M. Leenen, J. F. Schijven, F. M. Schets, J. C. Van der Vliet, F. Van Knapen, and A. M. De Roda Husman. 2014. "Quantitative Assessment of Infection Risk from Exposure to Waterborne Pathogens in Urban Floodwater." *Water Research* 48: 90–99. doi:10.1016/j.watres.2013.09.022.

Ellis, J. B., and D. O. Harrop. 1984. "Variations in Solids Loadings to Roadside Gully Pots." *Science of the Total Environment* 33 (1–4): 203–211. doi:10.1016/0048-9697(84)90394-2.

Fletcher, I. J., and C. J. Pratt 1981. "Mathematical Simulation of Pollutant Contributions to Urban Runoff from Roadside Gully Ponds." In *Proceedings of the 2nd International Conference on Urban Storm Drainage*. Urbana, USA.

Fulcher, G. A. 1994. "Urban Stormwater Quality from a Residential Catchment." *Science of the Total Environment* 146-147: 535–542. doi:10.1016/0048-9697(94)90279-8.

Gelhardt, L., M. Huber, and A. Welker. 2017. "Development of a Laboratory Method for the Comparison of Settling Processes of Road-Deposited Sediments with Artificial Test Material." *Water, Air, & Soil Pollution* 228 (12): 467. doi:https://doi-org.tudelft.idm.oclc.10.1007/s11270-017-3650-8.

Grottker, M. 1990. "Pollutant Removal by Gully Pots in Different Catchment Areas." *Science of the Total Environment* 93: 512–522.https://doi.org/10.1016/0048-9697(90)90142-H

Lager, J. A., W. G. Smith, W. G. Lynard, R. M. Finn, and E. J. Finnemore. 1977. *Urban Stormwater Management and Technology: Update and Users' Guide*. Cincinnati: U.S. EPA.

Langeveld, J. G., E. Liefting, and R. Schilperoort. 2016. *Regenwaterproject Almere* [Storm Water Project Almere]. Amersfoort: Stichting RIONED en STOWA.

Memon, F. A., and D. Butler. 2002. "Assessment of Gully Pot Management Strategies for Runoff Quality Control Using a Dynamic Model." *Science of the Total Environment* 295 (1–3): 115–129. doi:10.1016/S0048-9697(02)00056-6.

Naves, J., J. Rieckermann, L. Cea, J. Puertas, and J. Anta. 2020. "Global and Local Sensitivity Analysis to Improve the Understanding of Physically-based Urban Wash-off Models from High-resolution Laboratory Experiments." *Science of the Total Environment* 709. doi:10.1016/j.scitotenv.2019.136152.

Post, J. A. B., I. W. M. Pothof, J. Dirksen, E. J. Baars, J. G. Langeveld, and F. H. L. R. Clemens. 2016. "Monitoring and Statistical Modelling of Sedimentation in Gully Pots." *Water Research* 88: 245–256. doi:10.1016/j.watres.2015.10.021.

Pratt, C. J., and J. R. W. Adams. 1984. "Sediment Supply and Transmission via Roadside Gully Pots." *Science of the Total Environment* 33 (1–4): 213–224. doi:10.1016/0048-9697(84)90395-4.

Sansalone, J., J. J. Koran, J. M. Smithson, and S. G. Buchberger. 1998. "Physical Characteristics of Urban Roadway Solids Transported during Rain Events." *Journal of Environmental Engineering* 124 (5): 427–440. doi:10.1061/(ASCE)0733-9372(1998)124:5(427).

Sartor, J. D., and G. B. Boyd. 1972. *Water Pollution Aspects of Street Surface Contaminants*. Washington, DC: U.S.EPA.

Spekkers, M. H., M. Kok, F. H. L. R. Clemens, and J. A. E. Ten Veldhuis. 2013. "A Statistical Analysis of Insurance Damage Claims Related to Rainfall Extremes." *Hydrology & Earth System Sciences Discussions* 9 (10): 913–922. doi:10.5194/hess-17-913-2013.

Van Bijnen, M., H. Korving, J. G. Langeveld, and F. H. L. R. Clemens. 2018. "Quantitative Impact Assessment of Sewer Condition on Health Risk." *Water* 10 (3): 245–257. doi:10.3390/w10030245.

Viswanath, D. S., and G. Natarajan. 1989. *Data Book on the Viscosity of Liquids*. New York: Hemisphere Publishing Corporation.